J. Phys. D: Appl. Phys. 27 (1994) 970–978. Printed in the UK

The multi-avalanche nature of streamer formation in inhomogeneous fields

Matti Laan and Peeter Paris

Institute of Experimental Physics and Technology, University of Tartu, EE2400 Tartu, Estonia

Received 30 November 1993, in final form 9 March 1994

Abstract. The streamer formation in a positive point-plane gap both in air and nitrogen has been studied. The primary electrons were created by laser radiation. This gave the opportunity to initiate streamers in a wide range of voltages including the range of a steady corona in air as well as to determine the formative time lags. A streamer starts when the space charge density reaches a critical value in a spatially localized region. In a divergent field the streamer formation is preceded by the accumulation of space charge, i.e. it has a multi-avalanche nature. A model for calculation of formative time lags is presented. For a virgin gap the model describes fairly the accumulation process. For the voltage range of steady corona in air only the qualitative description of the mechanism is given.

1. Introduction

In a homogeneous field a streamer starts at voltages where the number of charge carriers of an avalanche $\exp(\int \alpha_0 dx)$ (α_0 = the first Townsend coefficient for Laplacian field) reaches a critical value $N_{cr} \sim 10^8$. In this case the field intensity of the space charge of ions becomes comparable to the intensity of the applied field. However it is possible to reach the same critical space charge field when a large number of avalanches develop within the diffusion radius of an avalanche. Thus the critical total number of carriers can be reached at lower fields as was demonstrated in experiments with α-particles [1, ch 5].

In inhomogeneous fields the streamer formation is possible at voltages where the mean number $\overline{N}$ of charge carriers of a single avalanche is less than 10^8. In that case the avalanche-to-streamer transition is explained by the stochastic nature of the avalanche growth [2], the larger avalanches ($N > \overline{N}$) grow into streamers. In a point-plane gap (hemispherical 0.1 cm in diameter point, gap spacing = 4 cm) in air the calculated number $\overline{N}$ for Laplacian field at the onset potential $U_0 \approx 8$ kV of a cathode-directed steamer is $\sim 10^4$; the development of an avalanche of $N \sim 10^8$ carriers has a very low probability [1, ch 3]. Such a large difference of $N_{cr}/\overline{N} \sim 10^4$ rather indicates that in a highly divergent field the streamer formation has a multi-avalanche nature: the critical conditions are achieved by the accumulation of the cloud of positive ions from several avalanches.

This paper describes the formation of a streamer without external triggering (a non-initiated streamer) as well as the formation of initiated streamers. Initiated streamers start due to a high number of primary electrons which are created by laser radiation. With this method of streamer initiation (i) the time moment and the place of liberation of primary electrons can be fixed, and (ii) the number of primary electrons can be varied easily. These factors allow the formative time lags to be determined as a function of voltage and the number of primary electrons.

2. Experimental set-up: methods

2.1. Discharge gap

A positive DC corona is studied in a point-plane gap (figure 1). The gap spacing is 4 cm, the point electrode is a hemispherically capped wire of diameter 0.1 cm. Points made of different materials (Pt, Al, Cu, Mo) are used. The plane electrode is an aluminium disc of diameter 20 cm with a probe electrode of diameter 1.5 cm in its centre. The point electrode is stressed. The stabilized power supply allows the voltage to be varied with a smallest step of 10 V.

2.2. Gases

Experiments are carried out in ambient air and in nitrogen. The discharge in nitrogen is studied in a stainless steel chamber. It is evacuated to 10^{-5} Torr with the help of an oil diffusion pump trapped by liquid nitrogen. The chamber is raised to 100 °C in a few hours and is then filled with nitrogen (99.996% N_2, the content of H_2O is less than 0.005 gm^{-3}) and the pressure is set at atmospheric pressure. In such a medium the 'ageing' of

0022-3727/94/050970+09$19.50

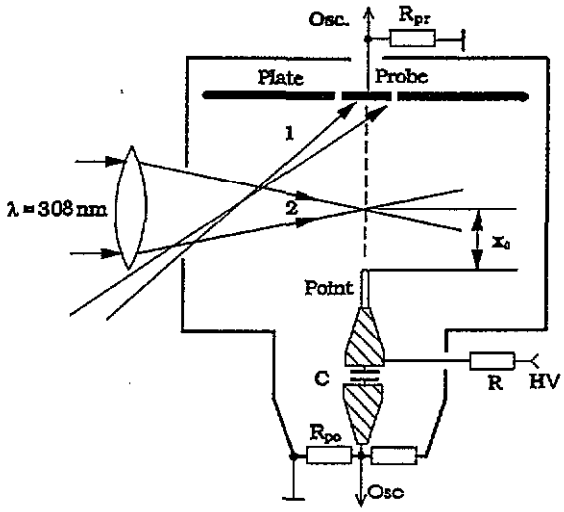

Figure 1. Experimental set-up. 1, primary electrons are released at the probe electrode; 2, primary electons are created at the gap axis by a focused laser beam. $R = 20$ kΩ, $C = 2000$ pF, $R_{po} = 50$, 470 Ω, $R_{pr} = 470$ Ω, 1.3 kΩ. HV, high voltage supply.

the gas takes place. There are two most striking effects of ageing:

(i) the current–voltage curve of a negative corona changes with time as previously described [3, 4],
(ii) recorded drift times of electrons from the cathode to anode decrease drastically with time.

It is known [5] that small traces of water vapour in nitrogen lead to an increase in the drift velocity. For this reason it is assumed that ageing is primarily caused by liberation of water vapour from the electrodes and the walls of the chamber. To reduce the influence of water vapour a bakeable trap with silica gel is set into the chamber. As a result the changes in the current–voltage curve of the negative corona slow down considerably and the drift velocity is maintained constant for a long time. Of course, the stabilization of discharge parameters may be caused by the absorption of other impurities (like the vapour of the diffusion pump oil) which are also absorbed by silica gel.

2.3. Primary electrons

Primary electrons are created by the radiation of excimer lasers wavelength ($\lambda = 308$ nm) which have different pulse lengths (10 ns and 100 ns) but nearly the same maximum pulse energy ≈ 100 mJ. The stepwise attenuation of laser radiation is carried out by means of calibrated grids. Two different ways for production of primary electrons are used:

(1) Electrons are released from the cathode by photo-effect: a divergent laser beam is directed to the probe electrode (figure 1, 1). To avoid side effects (like heating of the electrode surface) the illuminated area at the probe is ≈ 1 cm in diameter and the energy of a laser pulse does not exceed some millijoules. Changing the attenuation of laser radiation the number of released electrons varies from 10^6 to 10^7. The estimated order of magnitude of the coefficient of secondary emission γ is $\sim 10^{-8}$.
(2) Electrons are created by laser beam directed perpendicularly to the gap axis and focused on the gap axis at some distance x_0 from the point electrode (figure 1, 2). With transverse triggering one can neglect additional effects caused by the laser radiation at the electrodes. The maximum intensity I_m used near the beam focus does not exceed 5×10^{10} W cm^{-2}. The intensity I_m is considerably lower than that needed for optical breakdown ($I \sim 10^{12}$ W cm^{-2} for $\lambda = 350$ nm [6]). The total number of charge carriers released by a laser pulse is determined in a parallel plate gap of 1 cm spacing. The laser beam is focused to the mid-gap and the charge of current pulse in the gap circuit as a function of gap voltage is determined . From 1.5 to 3 kV the charge does not depend on voltage. From this value of charge the number of charge carriers is calculated. The number of charge carriers which corresponds to I_m both in air and nitrogen is nearly the same and has an order of magnitude of 10^8. The number of carriers created by a 10 ns pulse is somewhat less than that produced by a 100 ns pulse.

In air the distance x_0 is established with the accuracy of some tenths of a millimetre. Due to the laser instabilities the position of the focal point varies from pulse to pulse within the same limits. In the case of experiments in nitrogen the accuracy is less as experiments are carried out in the chamber and the direct measurement of x_0 is impossible. Besides this the role of laser instabilities in nitrogen is somewhat larger as the chamber is situated at a greater distance from the laser than the gap in air.

Near the beam focus the dimensions of the trace created by the radiation at a photo plate is $\approx 0.01 \times 0.02$ cm^2 and it remains nearly constant in limits of 0.6 cm along the beam axis. It is supposed that the ionization by laser radiation mostly takes place within this volume and thus the guessed value of the concentration of charged particles of a plasma ball in the beam focus is $\sim 10^{11}$ cm^{-3}. This concentration is high enough to lock electrons to ions as it is proved by the computer calculations [7], a plasma ball exists for a long time and only a small leak of electrons towards the anode occur. This viewpoint is also supported by our measurements (figure 9): the plasma ball is created by a 10 ns laser pulse but the duration of the flux of electrons to the anode exceeds 80 ns.

2.4. Measurements of current and time intervals

The DC is measured by an ammeter in the circuit of the plate and the probe connected in parallel . For the nanosecond resolution measurements of the current of streamer pulses a 350 MHz bandwidth oscilloscope of 50 Ω input resistance is used: a 50 Ω coaxial feedthrough [4] (figure 1, $R_{po} = 50$ Ω) is fitted with a 50 Ω transmission line. In the case of detecting low-current pulses (less than 10^{-4} A in height, see sections

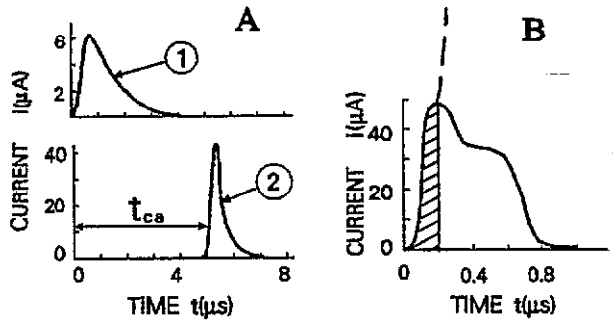

Figure 2. Sketches of current pulses. A: measurement of drift time t_{ca}. 1, current pulse in the probe circuit ($R_{pr} = 1.3$ kΩ; time constant $\tau = 1.5 \times 10^{-7}$ s); 2, current pulse in the point circuit ($R_{po} = 470$ Ω, $\tau = 5 \times 10^{-8}$ s). B: full curve, current pulse in the point circuit at $U > 8$ kV ($R = 50$ Ω); broken curve: current pulse of a streamer. The hatched area corresponds to the critical charge eN_{cr}.

3.1 and 3.2) in the probe and the point circuits the larger values of resistors are used (R_{po}, $R_{pr} = 470$ Ω, 1.3 kΩ), and signals are recorded by the help of an oscilloscope of 1 MΩ input resistance. Therefore the circuits are mismatched and the recorded signals are integrated.

The waveform of a laser pulse is recorded by a fast photodiode situated close to the discharge gap.

The time intervals are determined from the screen of oscilloscope. The time interval between the low-current pulses in the probe and the point circuits (drift time t_{ca}; see section 3.2, figure 2A) is measured with an accuracy of 0.05 μs. The time interval between the leading edges of laser pulse and streamer pulse (delay time t_d; see section 3.3) is measured with a higher precision. To achieve it a variable delay cable is switched in series with the photodiode. The accuracy of delay time measurements is 4 ns and it is determined mainly by the reproducibility of the adjustment of variable delay.

The light emitted by the discharge is detected by a fast photomultiplier and a static image intensifier.

2.5. Formulae for calculations

For computer calculations carried out by the Mathcad program various data are used. Numerical values of the constants in the expressions are given for our gap geometry; voltage U is in volts, pressure p is in Torr, distance x from the point tip is in cm.

The reduced field intensity E/p (V cm^{-1} Torr) along the gap axis is calculated according to the expression

$$E(x)/p = 3.6 \times 10^{-5} U (x + 0.05)^{-2} \exp[2(x + 0.05)].$$

Up to distance $x = 1$ cm it is a good fit [8] to the electric field distribution, obtained by the method of charge simulation [9]. At larger distances x the field is calculated according to the formula derived in [10] in hyperbolic approximation

$$E(x)/p \approx \frac{1}{p} \frac{1.4U}{x(2a - x) + (a - x)r}$$

$a = 4$ cm and $r = 0.05$ cm.

The ionization coefficient α is in cm^{-1}. The approximations from [11] are used:

$$\alpha/p = 8.6 \exp(-254/E/p) \qquad \text{for air}$$

$$\alpha/p = 8.8 \exp(-275/E/p) \qquad \text{for nitrogen.}$$

The drift velocity v_e of electrons is in cm s^{-1}. For air the expression from [13] is used

$$v = 10^6 (E/p)^{0.715}.$$

For nitrogen two different quadratic fits are derived: the first

$$v = 10^6 (0.27 + 0.471 E/p - (E/p)^2) \qquad E/p < 20$$

is based on experimental data from [14, ch 1], the other one

$$v = 10^6 [0.7 + 0.35 E/p - 5.64310^{-4} (E/p)^2]$$

is for higher fields and the data are from [15].

3. Results

3.1. Types of non-initiated positive corona

In air the sequence of different corona types does not differ from that described earlier by several investigators [15, ch 3]. The first detectable discharge type is a burst pulse which spreads along the point surface. It is possible to observe burst pulses about 200 V below the inception voltage U_0 of onset streamers. At voltages close to U_0 the amplitude of larger burst pulses achieves 0.1 mA and their duration is nearly 1 μs , the corresponding light pulse is shorter (≈ 70 ns) . At voltages $U > U_0$ both burst pulses and streamers exist. U_0 depends on humidity and pressure of ambient air and varies from 7.8 to 8.0 kV. No dependence on electrode material is mentioned. In the narrow range of voltage near the inception voltage the burst-to-streamer transition is observable: the steep current rise of a streamer pulse is preceded by a step. The recorded current waveform is very similar to the avalanche-to-streamer transition in a homogeneous field [1, ch 5]. The magnitude of the step is close to that of burst pulse and its duration does not exceed 20 ns. With the voltage increase the duration of step diminishes quickly and already 50 V above U_0 it is difficult to separate the step from the main pulse. The burst-to-streamer transition is described in more detail elsewhere [16]. The peak value of largest current pulses of streamers is 9 mA and their half width is ≈ 100 ns. The streamers are recorded in the range of ≈ 200 V. They have a branched structure and some branches develop up to 10 mm from the point. At higher voltages the discharge exists in the form of a steady glow, its current increases from 0.5 μA at 8.5 kV up to 9 μA at 14 kV.

In nitrogen the onset potential of the discharge is considerably higher: at 9.7 kV the first pulses of 0.25

μA in amplitude are recorded, their duration $\approx 10^{-6}$ s is determined by the time constant of the recording system. The number of electrons $N \geqslant 10^6$ in a pulse is close to the calculated number of charge carriers in an avalanche at this voltage. According to the static picture from several pulses (observed by the image intensifier) a large area of the hemispherical part of the point electrode is covered by a very faint luminous layer.

At 9.9 kV a steady discharge is established. With the voltage increase the DC current of steady discharge increases gradually from 1 μA at the onset up to 8 μA at 14 kV. At the point surface near its tip a more intensive luminous spot with sharp borders is observable. The area of the spot is $(1.2–1.5)10^{-4}$ cm^2 and above it a faint luminous channel extends far into the gap. From time to time the spot jumps to another place. Only few jumps per minute occur. The jump is accompanied by a sudden change of DC current (e.g. at $U = 10.1$ kV the current changes within the limits 1.8–2.2 μA) as well as by the streamer formation. It is difficult to say whether there are streamers also during the constant current or not. The height of the current pulse of a streamer vary from 16 to 20 mA and the halfwidth of pulses is ≈ 800 ns. By appearance the streamers are less if any branched than in air. The length of a non-branched channel varies within the limits 0.8–1.5 cm and the channel is often deflected from the gap axis, the branching occurs mainly at the end of the streamer channel.

In dry nitrogen the extinction voltage differs from the inception one: the steady discharge exists up to 8.7 kV. The extinction current of discharge is ≈ 0.12 μA. The same behaviour as at voltages above the inception voltage is observed: the sudden change of current is connected with a streamer formation, the length of streamer channel is diminishing with voltage decrease.

In non-dried nitrogen the extinction voltage equals to the inception one and the streamer is branched like in air.

3.2. Determination of drift times and ionization integral

Most of the experiments are carried out in nitrogen. The primary electrons are liberated from the probe by a 10 ns laser pulse.

The drift time t_{ca} is measured (figure 2A) as a function of voltage (figure 3). The results for dry nitrogen are close to that calculated on the bases of data from the literature (section 2.5). The presence of water vapour reduces drastically the drift time.

The numbers of electrons leaving the cathode N_c and reaching the anode N_a are determined from the areas $\int i\,dt$ of current pulses of the probe and the point, respectively. During their drift the number of electrons changes due to the losses as well as due to the ionization multiplication in a high field near the point. Up to 4 kV in dry nitrogen within the limits of experimental errors there is no difference between N_c and N_a (in non-dried nitrogen $N_a/N_c < 1$). As the value of the calculated ionization integral $\int \alpha_0 dx$ is close to one in

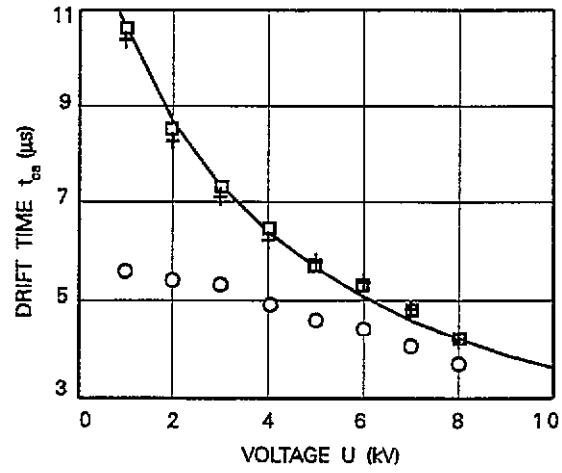

Figure 3. Drift time t_{ca} of electrons as a function of voltage. ○: non-dried nitrogen, 20 h after filling with fresh gas. + and □: dry nitrogen 100 h and 1 month, respectively, after filling. Full curve, the calculated dependence.

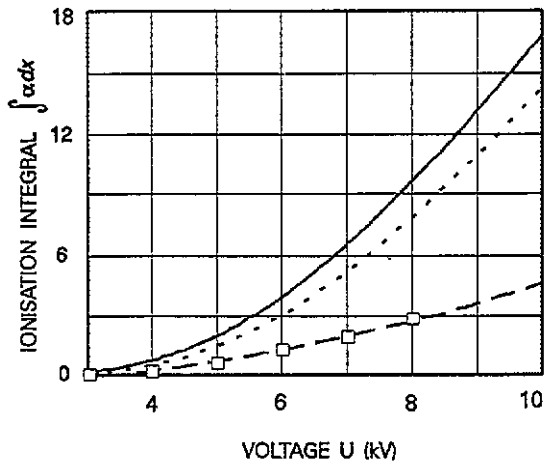

Figure 4. Ionization integral as a function of voltage. Full curve: air, Laplacian field. Dotted curve: nitrogen, Laplacian field. Curves for Laplacian field are calculated from the border of ionization zone. □: experimental results. Broken curve: a quadratic fit to experimental results.

this range of voltage it is possible to conclude that in this case the role of losses is negligible. At higher voltages ($U = 5–8$ kV) N_a increases with voltage but the waveform of current pulses does not change and the relation N_a/N_c does not depend on laser intensity. So the curve $\ln(N_a/N_c) = f(U)$ may be treated as a dependence for experimental ionization integral. In figure 4 the experimental points, a quadratic fit of

$$\ln(N_a/N_c) = \int \alpha dx = 5.2U^2 - 0.61$$

as well as the calculated curves $\int \alpha_0 dx = f(U)$ for a Laplacian field are presented.

At voltages $U > 8$ kV the waveform of current pulses of the point circuit changes. The simple waveform is replaced by a more complicated one (figure 2B): there is a higher hump at the beginning of a current pulse. At higher voltages from this hump a steep current rise starts (figure 2B) that corresponds to

streamer development as it is also confirmed by image intensifier observations. The onset voltage of an initiated streamer U_i depends on laser intensity: in the case of four-fold increase in intensity U_i diminishes from 8.7 kV to 8.2 kV. But independent of U_i there is a critical total number of charge carriers $N_{cr}^t = (2\text{–}5)\times 10^7$ (figure 2B) near the point which must be achieved by the moment of transition.

In the case of similar experiments in air the time interval between anode and cathode current pulses is nearly 3.5 ms and it corresponds to the drift time of negative ions. Using a hemispherical 1 mm point only large burst pulses are initiated in the region of onset streamers.

3.3. Measurements of delay times

Experiments are carried out in both ambient air and nitrogen. The primary electrons are created by a focused laser beam at the distance x_0 from the point. The long-pulse as well as the short-pulse laser are used, but the results do not depend remarkably on the pulse length. Delay time t_d needed for the start of an initiated streamer depends on voltage U, laser intensity I and distance x_0. Delay time is determined only for those values of x_0, I and U for which the jitter of t_d does not exceed some nanoseconds.

By appearance an initiated streamer has a branched structure, the length of branches increases with voltage increase. At higher laser intensities the branches developing towards the laser beam will prevail [17, 18].

In air the maximum distance is $x_0 = 0.8$ cm. At larger distances independent of laser intensities used the initiated streamers are not observed. For all distances under observation the behaviour of curves $t_d = f(U)$ is similar. The results for $x_0 = 0.5$ cm and for the long laser pulse are presented in figure 5. At every intensity I = constant below the inception voltage of non-initiated streamers U_0, the delay time decreases with the voltage increase and achieves its minimum near the potential U_0. Further increase in voltage also leads to an increase in delay time. In the region of steady corona the delay time remains nearly constant. At every voltage the decrease in intensity causes the increase in delay time.

In nitrogen the dependencies $t_d = f(U)$ are recorded up to a distance $x_0 = 1.6$ cm. This maximum distance is limited by the dimensions of viewport and not by the jitter of t_d. As in air the initiation of streamers is possible at voltages remarkably less than the inception voltage of non-initiated discharge. Compared with air the dependence on laser intensity at U = constant is considerably less. A typical curve of $t_d = f(U)$ is presented in figure 6: the delay time diminishes gradually as the voltage increase.

4. Discussion

A non-homogeneous discharge gap may be divided into two typical zones [19]: the drift zone and the ionization zone. In our gap at the voltages under observation, the border of the ionization zone x_i is at a distance < 0.06 cm from the point tip.

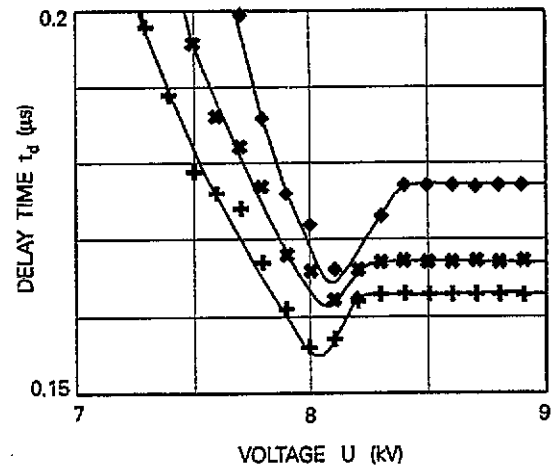

Figure 5. Delay time t_d in air as a function of voltage. Electrons are created at $x_0 = 0.5$ cm from the point. Voltage $U \approx 8$ kV corresponds to the onset of non-initiated streamers. +: laser intensity $I = I_m$. ×: $I = I_m/2$. ♦: $I = I_m/4$.

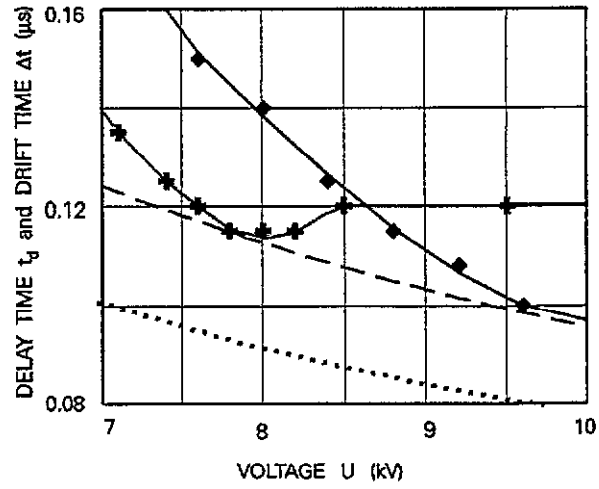

Figure 6. Delay time t_d and drift time Δt as a function of voltage. Electrons are created at $x_0 = 0.4$ cm. +: t_d in air. ♦: t_d in nitrogen. Dotted curve: calculated Δt for air. Broken curve: calculated Δt for nitrogen.

4.1. Feedback mechanism in nitrogen

Near the onset in air ($U \approx 8$ kV) the calculated (figure 4) size of an avalanche $\exp(\int \alpha_0 dx)$ is two orders of magnitude less than that at the onset potential ($U \approx 10$ kV) in nitrogen. At the same time, for a self-sustained discharge, the replenishment factor $\gamma \exp(\int \alpha_0 dx)$ must be 1 (γ = the coefficient of secondary emission). This means that compared with air the efficiency of secondary process(es) in nitrogen is much less. It is widely accepted that in air the different discharge forms (burst pulses, streamers, steady corona) are supported by the photoionization as a γ-mechanism, processes at the cathode play a minor role [15]. Only the results of experiments carried out in synthetic air [20] seem to prove that the development of the repetitive streamers is also supported by the cathode processes.

In nitrogen the photoionization is not so effective and the role of the cathode becomes dominant. This viewpoint is supported by different experimental

observations (see section 3.1):

(i) Instead of a luminous layer concentrated close to the point surface in the case of a steady corona in air, the channel of the steady state discharge in nitrogen extends far to the gap and, as was observed in purer conditions [21], the channel of a very weak luminosity bridges the gap. As a rule the channel of a steady discharge is deflected from the gap axis, most probably it starts from the edge of the probe where the field intensity is higher. Observed jumps of the DC current with corresponding replacement of the bright anode spot may be caused by a change in emissive site at the cathode.

(ii) The streamers in nitrogen are less branched and a non-branched channel is deflected from the gap axis like the channel of steady discharge. So it is probable that a streamer develops along the channel of a steady discharge, i.e. along the preionized path.

(iii) The difference between the inception and extinction voltages is not explainable supposing that the gas photoionization as a feedback mechanism of steady corona is dominant.

(iv) The detected current pulses at the onset of discharge correspond to single avalanches, i.e. a burst-pulse-like mechanism is not active.

So it is quite reasonable to assume that the steady discharge in nitrogen is a glow with its typical cathode region at the plane electrode, and the preionization ahead of a non-initiated streamer in nitrogen is caused rather by the background steady discharge than by the photoionization

4.2. Conditions for streamer formation

Multi-electron streamer initiation both in air and nitrogen is possible in a wide range of voltages including the case of low fields ($U_{cr}^{t} \approx 7$ kV) where the calculated number of the charge carriers of an avalanche is $\sim 10^2$ as well as in the region of steady corona. It is obvious that in all cases similar critical conditions must be established at the moment of streamer formation. Furthermore, these conditions must not differ from those for single electron initiation.

As has previously been demonstrated by experiments with α-particles in a homogeneous field [1], the streamer formation is determined rather by the critical density of charged particles than by the size of a single avalanche. In our experiments only the critical number of charge carriers $U_{cr}^{t} \sim 10^7$ near the point (see section 3.2) is directly determined. Due to the gap geometry most of charge carriers are created in a thin layer at the point surface. The area of this layer should not differ considerably from that for a non-initiated streamer. A non-initiated streamer in nitrogen (section 3.1) starts from an anode spot of $\sim 10^{-4}$ cm^2 in area. So an estimated critical value of the charge surface density is $\sigma_{cr} \sim 10^{-8}$ (C cm^{-2}). Calculated maximum field intensity ($E \sim 10^5$ V cm^{-1}) of the anode spot treated as a charged disc differs by less than 40% from the value of Laplacian field intensity at the point surface at the inception voltage ($U_0 \approx 8$ kV) of streamers in air. This result coincides with the general formulation of the criterion for streamer formation: a streamer starts when the intensity of the space charge field is close to that of applied field.

In the case of a steady corona in air the situation is more complicated. There are no problems with the achievement of a critical number of charge carriers as the point surface is covered by a laterally extended layer of ionized gas. According to the general analysis of corona stability [19] this type of discharge is stable as an accidental current increase will also enhance the positive space charge layer and thus weaken the field at the point, ionization is reduced and the original current is restored. The stability of steady discharge also follows from the analysis of its positive-slope I–U curve. For streamer formation the field at the cathode side of the layer must be high enough to ensure that ionization increases there. It becomes possible when in a spatially localized region of the layer the increase of ionization rate dn/dt for some reason occurs. It may lead to the spike-like extension of the region of ionized gas towards the cathode, i.e. a streamer forms. The cited model is supported by experimental results:

(i) In air a burst-pulse starts near the point tip and then due to the photoionization spreads over the point. During its development a space charge layer forms at the point surface. At $U > U_0$ a burst may grow into a streamer (section 3.1). The probability of transition is determined by the competition between the cathode-directed extension of ionization due to the accumulation of space charge in a limited area and the development of discharge to the lateral parts of the point. The last process diminishes the field at the cathode side of the layer and thus it lowers the probability of streamer formation. For this reason the transition always occurs at the initial part ($t < 20$ ns) of the burst as later the field is too weak to ensure the development of cathode-directed ionization instability.

(ii) It is possible to create streamers in the region of the steady corona in air (figure 5, $U > 8.5$ kV) where the point is covered by an extended ionized layer. In this case the local increase of dn/dt is caused by entering a large number of electrons created by a laser shot into the ionization zone in the limits of a small area.

(iii) Experiments with voltage pulses (1 kV in height and of 100 ns duration) superimposed to DC voltage demonstrate another possibility to create streamers in the steady corona region in air [17]. As a rule, a streamer starts from the lateral part of the layer where the layer is less homogeneous and so it is easier to achieve the local ionization instability.

Thus for streamer formation independent of the magnitude of Laplacian field and the initial distribution of the field, a critical space charge density must be achieved in a spatially localized region.

4.3. Interpretation of delay times

In [22] transverse triggering was also used and the experiments were carried out in similar conditions (point-plane gap, ambient air). In this paper the delay time t_d was interpreted as a time interval needed for streamer development from the anode to the cathode (the current pulses were recorded in the circuits of the probe and the outer part of the cathode), i.e. the drift time of the electrons to the ionization zone nor the final time interval required for the space charge accumulation were taken into account.

We shall present the measured delay time (section 3.3) as $t_d = \Delta t + t_f$. After

$$\Delta t = \int_{x_0}^{x_i} \frac{dx}{v(E(x)/p)}$$

the first electrons from a plasma ball at the distance x_0 reach the border of ionization zone at x_i and t_f (formative time) is the time interval needed for the accumulation of critical space charge in the ionization zone. The measured values of t_d and the calculated values of Δt as a function of voltage both for air and nitrogen are presented in figure 6. As one can see:

(i) even in the case of large number of primary electrons and at the onset of streamers in air ($U \approx 8$ kV) an accumulation period precedes the streamer formation,
(ii) formative time $t_f = t_d - \Delta t$ in the region of steady corona in air increases with the voltage increase,
(iii)in nitrogen t_f diminishes with voltage increase and it is close to zero at the onset of non-initiated discharge.

4.4. Model of space charge accumulation

The model describes the space charge accumulation in a virgin gap only and so the streamer formation in the region of the steady corona is not treated here.

We assume that during the formative time t_f the flux of electrons $n_{ei}v_{ei}$ into the ionization zone is constant (n_{ei}, v_{ei} are, respectively, the concentration and the velocity of electrons at x_i). Most of the electrons enter the ionization zone within the limits of a small area δS. In the ionization zone the number of charge carriers N increases and during the time interval $\delta t N(\delta t) = n_{ei}v_{ei}\delta t \delta S \exp(\int \alpha dx)$ positive ions accumulate inside a thin disc-like volume situated close to the point surface. It is supposed that the ions are immovable during the accumulation.

During the accumulation the ionization coefficient changes due to the space charge effects. The space charge causes the redistribution of the total field and α decreases [1, ch 3]. According to recent studies [23] in a homogeneous field at $E/p = 37$ V cm^{-1} Torr, the avalanche growth retards when the surface density of primary electrons is higher than 10^8 cm^{-2}. In our experiments the estimated density of primary electrons at x_i exceeds this value and that is why the experimental ionization integral $\int \alpha dx$ is lower than that

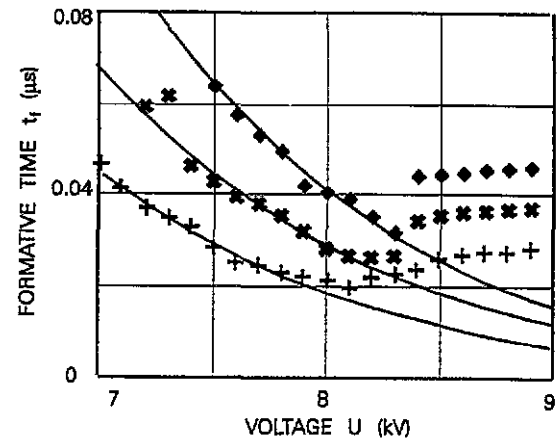

Figure 7. Formative time t_f in air as a function of voltage. Electrons are created at $x_0 = 0.3$ cm. Full curves are calculated according to the model. +: $l = l_m$, the full curve corresponds to $n_{ei} = 2.8 \times 10^{10}$ cm^{-3}. ×: $l = l_m/4$, $n_{ei} = 1.85 \times 10^{10}$ cm^{-3}. ♦: $l = l_m/8$, $n_{ei} = 1.26 \times 10^{10}$ cm^{-3}.

for a Laplacian field (figure 4). The actual smooth dependence of $\int \alpha(x,t)dx$ on time is unknown and it is replaced by a step-wise one: at the initial stage of accumulation the ionization occurs in Laplacian field, at the later stage the ionization is governed by $\int \alpha dx$ (figure 4). Furthermore, we suppose that there is no remarkable difference in $\int \alpha dx$ for air and nitrogen. The estimated duration of the initial stage is very short compared with that of t_f, e.g. at $U \approx 8$ kV and $n_{ei} \sim 10^{10}$ cm^{-3} (this value of n_{ei} corresponds to our experimental conditions (figure 8)) the time interval for accumulation of 10^6 charge carriers is less than 1 ns.

After a formative time t_f the surface density $eN/\delta S$ (e = elementary charge) of space charge layer reaches its critical value σ_{cr} (section 4.2) and a streamer forms. Thus according to this rough model the formative times are calculated as

$$t_f(U, n_{ei}) = \frac{\sigma_{cr}}{en_{ei}v_{ei}\exp(\int \alpha dx)}.$$

In this expression the concentration n_{ei} is a free parameter and its value has been chosen to achieve the best coincidence of the model with the experimental results.

The curves $t_f = f(U)$ ($x_0 = 3$ mm) for air and for various laser intensities are presented in figure 7. Within the limits of its validity (i.e. at voltages below the onset of steady corona) the model describes fairly well the accumulation process. It is likely that the increase in t_f in the voltage range of steady corona is caused by the decrease in the field at the cathode side of the ionized layer; thus for achievement of the critical field there, longer formative times are needed.

For all distances $x_0 > 2$ mm the coincidence with experimental results is similar. If the electrons are released closer to the point the experimental values of t_f are systematically longer than predicted by the model. This may be caused by the field reduction near the plasma ball created by the laser radiation: according

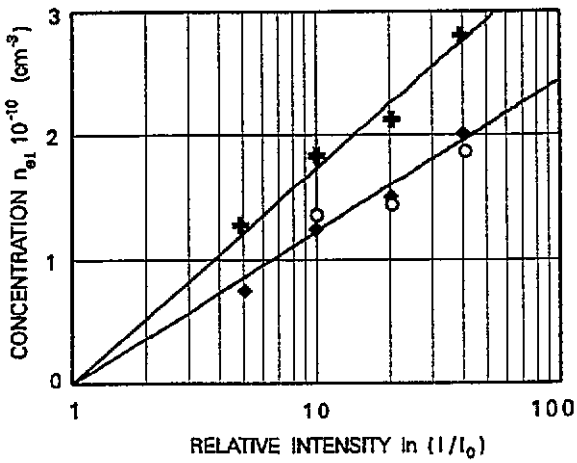

Figure 8. Concentration n_{ei} at the border of ionization zone as a function of relative laser intensity. +: electrons are created at $x_0 = 0.3$ cm. ♦: $x_0 = 0.4$ cm. ○: $x_0 = 0.5$ cm.

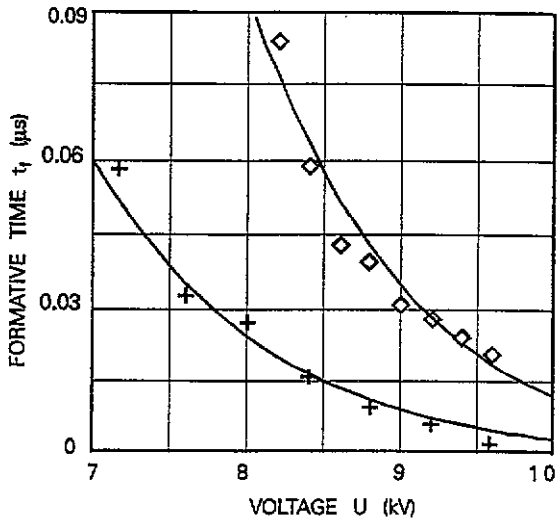

Figure 9. Formative time t_f in nitrogen as a function of voltage. Full curves are calculated according to the model. Electrons are created at $x_0 = 0.4$ cm. +: 100 ns laser pulse, full curve corresponds to $n_{ei} = 2.2 \times 10^{10}$ cm^{-3}. ◊: 10 ns laser pulse, $n_{ei} = 0.6 \times 10^{10}$ cm^{-3}.

to [18] the streamer branches never pass through the position of plasma ball.

The concentration of electrons n_{ei} reaching the ionization zone varies in limits $(0.5–3) \times 10^{10}$ cm^{-3}, i.e. approxmately 10^5 electrons per nanosecond pass the area $\delta S = 10^{-4}$ cm^2 at the border of the ionization zone. In figure 8 the dependencies $n_{ei} = F(I)$ for different x_0 in air are presented. The concentration n_{ei} logarithmically depends on laser intensity $n_{ei} = A \ln(I/I_0)$, the constant I_0 has a simple physical explanation: it is the minimum laser intensity which is able to ionize the gas and its estimated order of magnitude is $\sim 10^8$ W cm^2 (the corresponding energy of laser pulse is ≈ 2 mJ). The slope A is different for different x_0: it describes the decrease of the number of electrons due to attachment during their drift towards the point.

The dependencies $t_f = f(U)$ ($x_0 = 4$ mm) for nitrogen are presented in figure 9. The calculated curves are close to the points determined from the experiment for the whole range of voltage under observation.

There are several unsolved problems in this field. Some of these (the most exciting for us) are:

(i) The actual spatial distribution of charge carriers near the point during the space charge accumulation.
(ii) The mechanism of streamer formation in the case of steady corona.
(iii) The mechanism of non-initiated streamer formation and development during the sudden change of current of steady discharge in nitrogen.

5. Conclusions

It has been proved experimentally that in the case of a large number of primary electrons a streamer forms at voltages considerably lower than the inception voltage as well as in the range of steady corona.

For streamer formation an ionization instability must develop in a spatially localized region. The local increase in ionization leads to an increase in the space charge field in this region. A streamer starts when the space charge field achieves a critical value. These conditions are common in different experimental conditions.

At the inception voltage of streamers in a homogeneous field the number of charge carriers of a single avalanche is high enough to reach the critical field but if the gap is undervolted a large amount of primary electrons and/or an accumulation period of space charge are needed for streamer formation.

In a highly divergent field in air even at the inception voltage a space charge accumulation precedes the streamer formation as the number of charge carriers of an avalanche is much less than the critical number and so the streamer formation has a multi-avalanche nature. The increase of the inception voltage in nitrogen is caused by the low value of secondary emission coefficient.

Acknowledgments

One of the authors (ML), would like to thank Professor R S Sigmond for discussions on the problems of stability of corona discharges during his stay at the Norwegian Institute of Technology. The authors would like to thank Svein Sigmond for very useful discussions as well as the Norwegian Scientific Foundation (NAVF) for their scholarship. The study was supported by the Estonian Scientific Foundation.

References

[1] Raether H 1964 *Electron Avalances and Breakdown in Gases* (London: Butterworths)
[2] Pedersen A 1989 On the electrical breakdown of gaseous dielectrics *IEEE Trans. Electr. Insulation* **24** 721–39
[3] Laan M, Paris P and Perelygin V 1991 Laser action on corona pulses *Acta Phys. Slov.* **42** 91–7

[4] Korge H, Laan M and Paris P 1993 On the formation of negative coronas *J. Phys. D: Appl. Phys.* **26** 231–6
[5] McDaniel E W 1964 *Collision Phenomena in Ionized Gases* (New York: Wiley) ch 11
[6] Rosen D I and Weil G 1987 Laser induced breakdown in nitrogen and rare gases at 0.53 and 0.35 μm *J. Phys. D: Appl. Phys.* **20** 1264–76
[7] Morrow R and Lowke J J 1981 Space-charge effects on drift dominated electron and plasma motion *J. Phys. D: Appl. Phys.* **14** 2027–34
[8] Abou-Seada M S 1980 Calculation of the high-frequency breakdown voltages of point-plane air gaps *IEEE IAS 15th Annual Meeting* pp 1118–22
[9] Abou-Seada M S and Nasser E 1969 Digital computer calculation of the potential and its gradient of a twin cylindrical conductor *IEEE Trans. PAS* **88** 1802–14
[10] Coelho R and Debeau J 1971 Properties of the tip-plane configuration *J. Phys. D: Appl. Phys.* **4** 1266–80
[11] Granovski V L 1971 *Electrical Current in Gas* (Moscow: Nauka) ch 2 (in Russian)
[12] Sigmond R S 1983 Basic corona phenomena: the role of space charge saturation and secondary streamers in breakdown *16th Int. Conf. on Phenomena in Ionized Gases (Düsseldorf)* Invited papers 174–86
[13] Brown S 1959 Basic data on plasma physics
[14] Wetzer J M and Wen L 1991 Different avalance types in electronegative gases *J. Phys. D: Appl. Phys.* **24** 1964–73
[15] Loeb L B 1965 *Electrical Coronas* (Berkeley, CA: University of California Press)
[16] Laan M and Paris P 1992 Streamer initiation by x-ray pulse *Acta et Comment. Univ. Tartuensis: Methods of Study of Electrical Processes in Gases and Aerosols* **950** 14–22
[17] Laan M and Paris P 1992 Formation of corona pulses *9th Symp. on Elementary Processes and Chemical Reactions in Low Temperature Plasmas* (Slovakia: Small Carpathy) Invited papers 201–16
[18] Paris P, Aints M and Haljaste A 1993 Development of a laser-initiated streamer *21st Int. Conf. on Phenomena in Ionized Gases (Bochum, Germany)* vol II pp 263–4
[19] Sigmond R S and Goldman M 1982 Corona discharge physics and applications *Electrical Breakdown and Discharges in Gases* part B, ed E E Kunhardt and L H Luessen (New York: Plenum) pp 1–64
[20] Kondo K and Ikuta N 1981 Highly resolved observation of the primary wave emission in atmospheric positive-streamer corona *J. Phys. D: Appl. Phys.* **13** L33–L38
[21] Korge H, Kudu K and Laan M 1979 The discharge in pure nitrogen at atmospheric pressure in point-to-plane discharge gap *3rd Int. Symp. on High Voltage Engineering (Milan)* paper 31.04
[22] Soulem N, Pignolet P, Peyrous R, Held B and Loiseau J F 1992 Laser investigation of positive point-to-plane discharge ambient air *10th Int. Conf. on Gas Discharges and their Applications (Swansea)* vol 1 pp 286–9
[23] Kennedy J T, Wetzer J M and van der Laan P C T 1992 Experimental study of space charge effects in avalanches in atmospheric nitrogen *10th Int. Conf. on Gas Discharges and their Applications (Swansea)* vol 1 pp 516–19